Int. J. Nanoelectronics and Materials **9** (2016) 37-49

# Synthesis, Structural, Surface Morphology, Optical and Electrical Properties of Silver Oxide Nanoparticles

*Suresh Sagadevan**

*Department of physics, Sree Sastha Institute of Engineering and Technology, Chennai-600 123, India.*

Received 17 Jan. 2015; Revised 7 April 2015; Accepted 28 May 2015

## Abstract

Silver oxide ($Ag_2O$) nanoparticles were synthesized using a wet chemical technique. The synthesized nanoparticles were investigated by X-ray diffraction analysis (XRD), scanning electron microscopy (SEM), transmission electron microscopy (TEM), UV analysis and dielectric studies. The powder X-ray diffraction (XRD) shows that face-centered cube structure of silver oxide and the average crystallite sizes were calculated to be 18.6 nm. The particle size and morphology were studied using the scanning electron microscope (SEM) and transmission electron microscopy (TEM). The UV-Visible absorption spectrum analyzing showed the strong absorption peak and nearly transparent nature of the particle at visible region. The wide range of band gap energy value was found to be 4.70 eV. The dielectric properties of silver oxide nanoparticles were studied in the frequency range of 50 Hz–5 MHz at different temperatures. The frequency dependence of the dielectric constant and dielectric loss is found to decrease with an increase in the frequency at different temperatures. Further, electronic properties, such as valence electron plasma energy, average energy gap or Penn gap, Fermi energy and electronic polarizability of the silver oxide nanoparticles were calculated. AC electrical conductivity measurement was studied.

**Keywords:** XRD, SEM, TEM, UV analysis, Dielectric constant and Dielectric loss

## 1. Introduction

Synthesis of nanomaterials with controlled morphology, size, chemical composition, and crystal structure, and in large quantity, is a key step toward nanotechnological applications. Nanostructured materials have attracted the attention of researchers not only by their unique chemical and physical properties but also by their potential application in many fields, which has stimulated the search for new synthetic methods for these materials. These materials consist of small grains with sizes below 100 nm. Metal oxide nanoparticles have attracted a great deal of attention from researchers for both their fundamental size-dependent optoelectronic properties and their wide range of applications [1]. Silver oxide nanostructures have attracted significant consideration because of their potential application in fabricating nano-scale electronics, optical to biological micro-devices, electron field

*) For Correspondence;E-mail: sureshsagadevan@gmail.com

emission sources for emission displays, and the surface electron field emission sources for emission displays, and the surface enhanced Raman property with controlled shape and morphology [2-6]. It displays wide group of derivatives ($Ag_2O$, $Ag_2O_3$, and $Ag_3O_4$ etc) that attracted considerable attention, mainly owing to the widespread uses of oxides. In nanotechnology and nano-structural materials, sensors have been playing a major role in the development of very accurate, highly-sensitive, and reliable devices. Silver oxide nanocrystals and thin films have been intensively pursued for promising applications such as photovoltaic materials, important components in optical memories and plasmon photonic devices [7-9]. Silver oxides crystallize in different types of crystal structures, leading to a variety of interesting physicochemical properties such as electronic, optical, catalytic and electrochemical properties. Among various chemical synthesis methods for preparation of metal oxides of large surface area, a sol-gel process offers several advantages over other methods, better homogeneity, controlled stoichiometry, high-purity, phase-pure powders at a lower temperature and flexibility of forming dense monoliths, thin films or nanoparticles. Sol-gel method is widely applied in preparation of nano- $Ag_2O$ powder. Usually, heat posttreatment at high temperature is necessary for removal of organic compounds and to acquire perfect nanocrystalline $Ag_2O$. However, it is very difficult to maintain the nanometric-scale structure of a material when it is subjected to heat-treatments. The heat-treatments steps are fundamental to achieve an optimal combination of mechanical, catalytic and electronic properties. This paper deals with the preparation of silver oxide nanoparticles using the wet chemical method. The prepared nanoparticles were characterized by powder X-ray diffraction analysis, SEM, TEM, UV-analysis and dielectric studies.

## 2. Experimental procedure

Nanoparticles of silver oxide were synthesized by wet chemical method. The chemicals such as silver nitrate and urea were used as the precursor materials to prepare silver oxide nanoparticles. Silver nitrate and urea was dissolved in de-ionized water and stirred well by magnetic stirrer for 30 min. Ammonia solution was added drop wise into the solution. Then the mixture has been placed onto the hot-plate with stirring for 6 hours. The prepared silver oxide was washed with acetone and dried. After drying, nanoparticles were grinded to obtain a fine powder for characterization. The development of silver oxide nanoparticles can be well explained based on the chemical reactions concerned and crystal growth behaviors of silver oxide. For the synthesis of silver oxide nanoparticles, silver nitrate (AgNO3) and NH4OH (in presence of surfactants & urea) were mixed under continuous stirring at 120ºC. During growth of silver oxide nanoparticle, surfactant is used to control the size, which has significant role in reaction systems.

## 3. Characterization Techniques

The prepared nanoparticles were characterized by powder X-ray diffraction analysis, SEM, TEM, UV-analysis and dielectric studies. The XRD pattern of the silver oxide nanoparticles was recorded by using a powder X-ray diffractometer (Schimadzu model: XRD 6000 using CuKα (λ=0.154 nm) radiation, with a diffraction angle between 20 to 70°. The crystallite size was determined from the broadenings of corresponding X-ray spectral peaks by using Debye Scherrer's formula. Scanning Electron Microscopy (SEM) studies were carried out on JEOL, JSM- 67001. TEM images were taken using a TEM CM200 with an accelerating voltage of 200 kV. The optical absorption spectrum of the silver oxide nanoparticles has been taken by using the VARIAN CARY MODEL 5000

spectrophotometer in the wavelength range of 300 – 800 nm. The dielectric properties of the silver oxide nanoparticles were analyzed using a HIOKI 3532-50 LCR HITESTER over the frequency range 50Hz-5MHz.

## 4. Results and discussion

In order to find out the size and to study the structural properties of the synthesized silver oxide nanoparticles, the powder XRD analysis was performed. Structural identification of silver oxide nanoparticles were carried out with X-ray diffraction in the range of angle $2\theta$ between 20º to 70º. Fig.1 shows the XRD patterns for silver oxide nanoparticles, which were nanocrystalline in nature. It is clearly revealed that all of the peaks match well with the face-centered cube structure and the three sharp peaks (111), (200), and (220) indices respectively. The three diffraction peaks can be readily indexed to the (111), (200), and (220) planes of FCC silver. Hence, all the reflected peaks in this pattern were found to match with the silver oxide phase having face centered cube (FCC). The broadened peak shows the nanometer-sized crystallites. The average nano-crystalline size (D) was calculated using the Debye-Scherrer formula,

$$D = \frac{0.9\lambda}{\beta \cos\theta} \tag{1}$$

where λ is the X-ray wavelength (CuKα radiation and equals to 0.154 nm), θ is the Bragg diffraction angle, and β is the FWHM of the XRD peak appearing at the diffraction angle θ. The average crystalline size is calculated from X-ray line broadening using Debye-Scherrer equation to be about 18.6 nm.

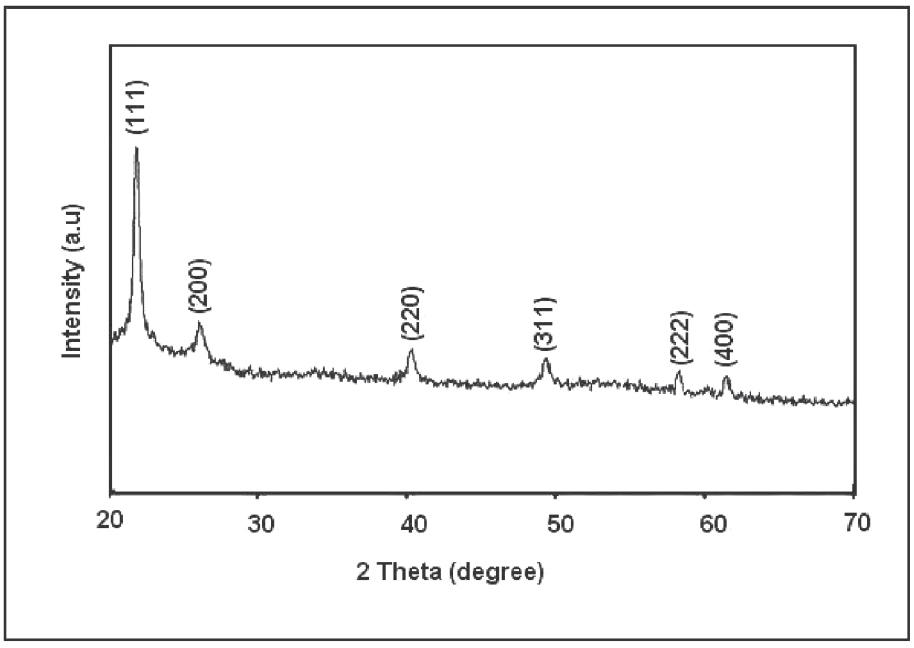


Fig. 1: X-ray diffraction patterns of silver oxide nanoparticles

Scanning electron microscopy (SEM) is giving morphological examination with direct visualization. The techniques based on electron microscopy offer several advantages in morphological and sizing analysis; however, they provide limited information about the

size distribution. For SEM characterization, nanoparticles solution should be first converted into a dry powder, which is then mounted on a sample holder followed by coating with a conductive metal, such as gold, using a sputter coater. The sample is then scanned with a focused fine beam of electrons. The surface characteristics of the sample are obtained from the secondary electrons emitted from the sample surface. The morphology of the silver oxide nanoparticles is shown in Fig.2. From the image, it is clear that the particles were highly agglomerated in nature. The SEM pictures clearly show randomly distributed grains with smaller size. From the SEM analyses, one can conclude the formation of nanoparticles spherical structure. Here it is grown in very high-density and possessing almost uniform spherical shapes. The image reveals that the average size of the particles is 18.3 nm.

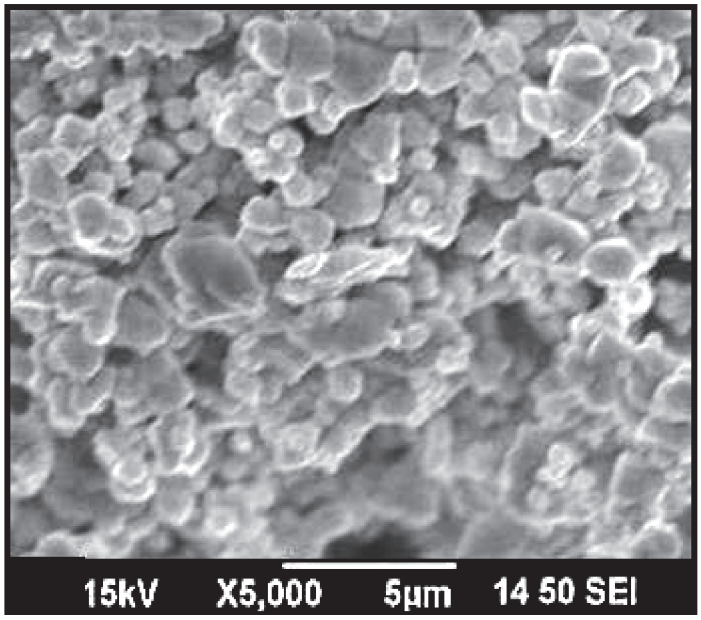


Fig.2: SEM image of nanoparticles

The transmission electron microscope utilized a high energy electron beam transmitted through a very thin sample to image and analyze the microstructure of materials with atomic scale resolution. The electrons are focused with electromagnetic lenses and the image is observed on a fluorescent screen, or recorded on film or digital camera. The electrons are accelerated at several hundred kV, giving wavelengths much smaller than that of light: 200kV electrons have a wavelength of 0.025Å. Whereas, the resolution of the optical microscope is limited by the wavelength of light, that of the electron microscope is limited by aberrations inherent in electromagnetic lenses, to about 1–2 Å. Transmission electron microscope is used to characterize the microstructure of materials with very high spatial resolution. The transmission electron microscopic study was carried out to confirm the actual size of the particles, their growth pattern and the distribution of the crystallites. TEM image of the synthesized silver oxide nanoparticles is shown in Fig.3. As can be seen from the TEM image, the particles are nearly spherical shapes with well defined boundaries. It is evident from the micrographs that the average size of the particles as directly measured from the image is ~19 nm. This result is similar to that obtained from XRD analysis.

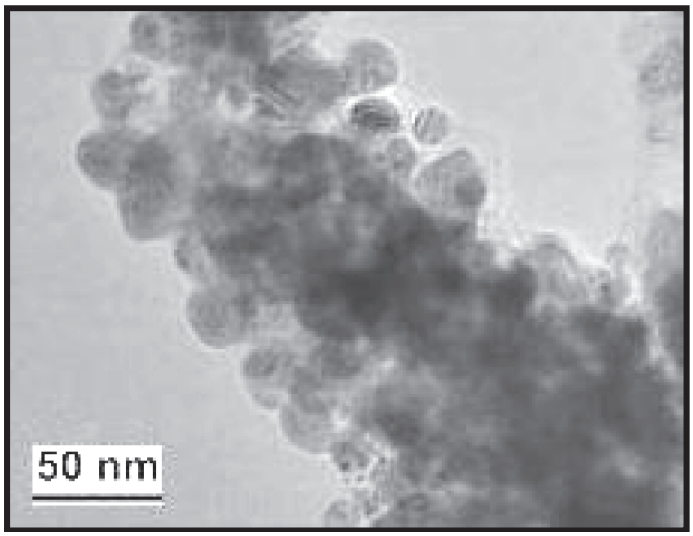


Fig .3: TEM image of silver oxide nanoparticles

Optical absorption study was carried out on silver oxide nanoparticles. In UV-visible absorption spectrum, the outer electrons of atoms or molecules are absorbed by the radiant energy and undergo transitions to higher energy levels. In this phenomenon, the spectrum obtained due to optical absorption can be analyzed to acquire the energy band gap of the metal oxides. For UV-visible absorption spectrum of silver oxide nanoparticles solution is measured as a function of wavelength, which is shown in Fig.4. The spectrum gives information about the structure of the molecule because the absorption of UV and visible light involves promotion of the electron in the $\sigma$ and $\pi$ orbital from the ground state to higher states. The optical absorption coefficient was calculated in the wavelength range of 200 - 800 nm. The absorption edge was obtained at a shorter wavelength. The value of the absorption edge of nanoparticles is 265 nm. Hence, the absorption edge of the products obtained by us exhibits a large blue-shift, which is attributed to the quantum confinement of charge carriers in the nanomicrocrystals. The silver oxide nanoparticles have excellent transmission in the entire visible region. The lower cutoff wavelength is 265 nm is mainly used in optical applications and hence optical transmittance window and the transparency lower cut off (200 nm-400 nm). This transparent nature in the visible region is a desirous property for the material used for optoelectronic device applications. It shows that the silver oxide nanoparticles has a good transparency in UV, visible and near IR region indicating that it can be used for device applications.

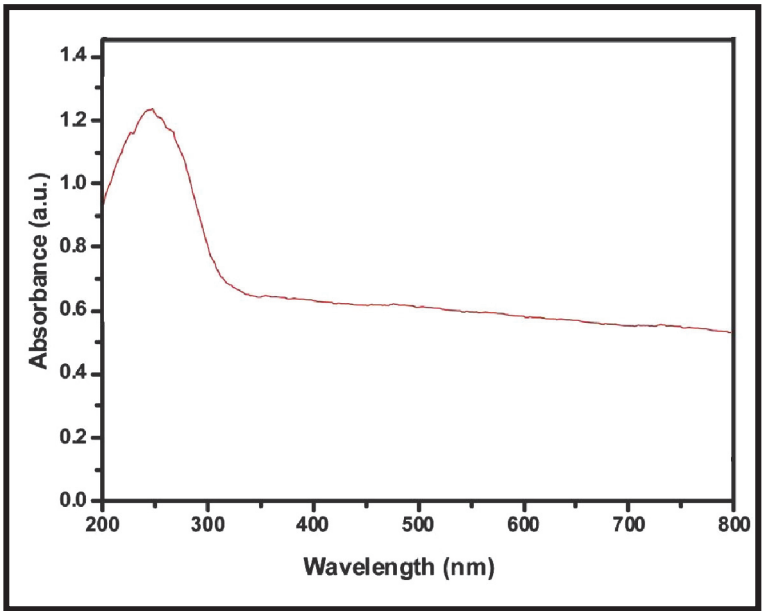


Fig.4: Optical absorption spectrum of silver oxide nanoparticles

The optical absorption coefficient (α) has been calculated from transmittance using the following relation

$$\alpha = \frac{1}{d}\log\left(\frac{1}{T}\right) \tag{2}$$

where T is the transmittance and d is the thickness. The study has an absorption coefficient (α) obeying the following relation for high photon energies (hν)

$$\alpha = \frac{A(h\nu - E_g)^{1/2}}{h\nu} \tag{3}$$

where $\alpha$, $E_g$ and $A$ are the absorption coefficient, band gap and constant respectively. By extrapolating the linear region in the plots of versus $(\alpha h\nu)^2$ versus hν is shown in Fig.5, the band gap value is estimated as 4.70 eV. This high value of band gap indicates that the silver nanoparticles possess dielectric behavior to induce polarization when powerful radiation is incident on the material. The absence of absorption bands in the visible region and the wide band gap of the silver oxide nanoparticles confirm to the suitability for photonic and optical applications. The larger energy band gap shows that the defect concentration in the silver oxide nanoparticles is very low.

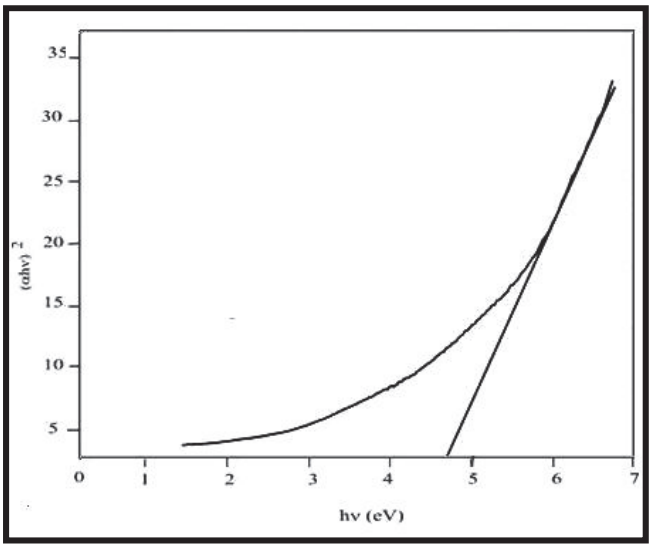


Fig.5: Plot of $(\alpha h\nu)^2$ Vs photon energy

The dielectric constant and the dielectric loss of the 10 mm in diameter pellet have been used for the determination of dielectric properties of silver oxide nanoparticles. The corresponding thickness of the pellet was 1.20 mm was studied at different temperature using a HIOKI 3532-50 LCR HITESTER in the frequency range of 50 Hz to 5 MHz. The results of the dielectric constant and dielectric loss as a function of frequency have been plotted in Figs. 6&7. It can be easily interpreted from the plots that the silver oxide nanoparticles show same trend, as having high values of dielectric constant and dielectric loss at low frequencies and decrease with the increase in frequency while reaching to a constant saturated value at high frequencies, depicting a frequency independent behavior. These defects activate interfacial polarizations at low frequencies. Due to this polarization, the dielectric constant is higher at low frequencies. The net polarization of silver oxide is owing to ionic, electronic, dipolar and space charge polarizations [10]. The huge value of the dielectric constant is due to the fact that silver oxide acts as a nanodipole under electric fields [11]. The small-sized particles require a large number of particles per unit volume, important in an increase of the dipole moment per unit volume, and a high dielectric constant. The dielectric constant at low frequencies starts from high value and decreases with increase in temperature. As the temperature increases, the dielectric constant values start increasing. The high value of dielectric constant at low temperature credited to space charge polarization whereas at higher temperature and at low frequencies it possibly connected with defect related conduction processes [12].

The variations of dielectric loss of silver oxide nanoparticles of with frequency and temperature are shown in Fig.7. It can be seen that dielectric loss decreases with increase of frequency and at higher frequencies the loss angle has almost the same value at all temperatures. In dielectric materials, generally dielectric losses take place due to absorption current. The orientation of molecules along the direction of the applied electric field in polar dielectrics requires a part of electric energy to overcome the forces of internal friction [13]. One more part of electric energy is utilized for rotations of dipolar molecules and other kinds of molecular transfer from one position to another, which also involve energy losses. In nanophase materials, inhomogeneities similar to defects and space charge formation in the inter phase layers create an absorption current ensuing in a dielectric loss [14].

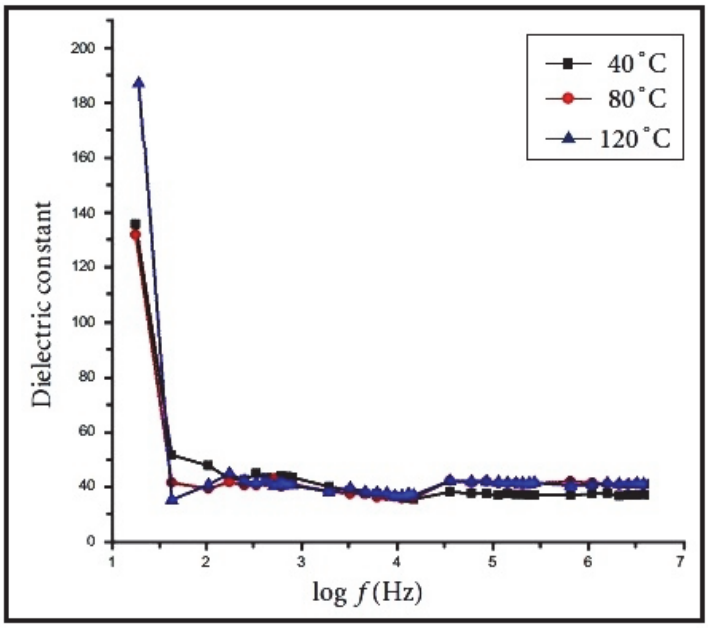


Fig. 6: Dielectric constant as a function of log frequency

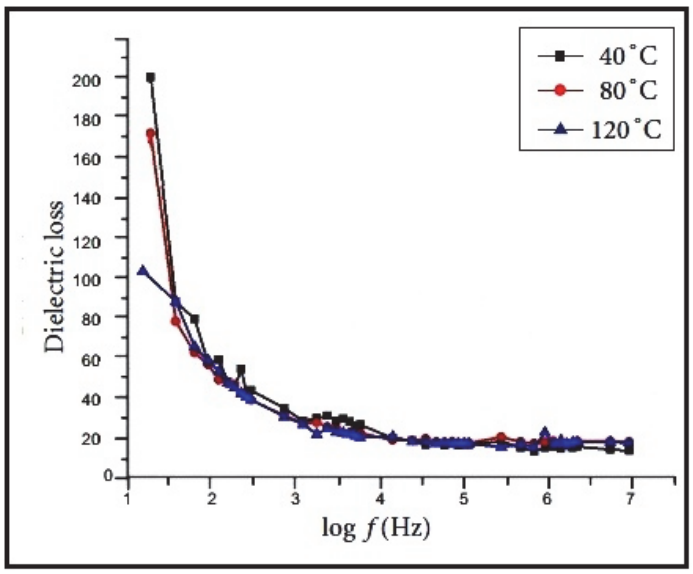


Fig. 7: Dielectric loss as a function of log frequency

In the proposed relation, only one parameter viz, the high frequency dielectric constant is required as input, to evaluate electronic properties like valence electron plasma energy, average energy gap or Penn gap, Fermi energy and electronic polarizability of the silver oxide nanoparticles. The theoretical calculations show that the high frequency dielectric constant is explicitly dependent on the valence electron Plasma energy, an average energy gap referred to as the Penn gap and Fermi energy. The Penn gap is determined by fitting the dielectric constant with the Plasmon energy [15], the Penn gap is determined. The following relation [16] is used to calculate the valence electron plasma energy, $\hbar\omega_p$

$$\hbar\omega_P = 28.8\left(\frac{Z\rho}{M}\right)^{1/2} \tag{4}$$

According to the Penn model [17], the average energy gap for the silver oxide nanoparticles is given by

$$E_P = \frac{\hbar\omega_P}{(\varepsilon_\infty - 1)^{1/2}} \tag{5}$$

where $\hbar\omega_P$ is the valence electron plasmon energy and the Fermi energy [15] given by

$$E_F = 0.2948(\hbar\omega_P)^{4/3} \tag{6}$$

Then, the electronic polarizability α, using a relation [18, 19],

$$\alpha = \left[\frac{(\hbar\omega_P)^2 S_0}{(\hbar\omega_P)^2 S_0 + 3E_P^2}\right] \times \frac{M}{\rho} \times 0.396 \times 10^{-24} cm^3 \tag{7}$$

where $S_0$ is a constant given by

$$S_0 = 1 - \left[\frac{E_P}{4E_F}\right] + \frac{1}{3}\left[\frac{E_P}{4E_F}\right]^2 \tag{8}$$

The Clausius-Mossotti relation,

$$\alpha = \frac{3}{4}\frac{M}{\pi N_a \rho}\left[\frac{\varepsilon_\infty - 1}{\varepsilon_\infty + 2}\right] \tag{9}$$

The following empirical relationship is also used to calculate polarizability (α),

$$\alpha = \left[1 - \frac{\sqrt{E_g}}{4.06}\right] \times \frac{M}{\rho} \times 0.396 \times 10^{-24} cm^3 \tag{10}$$

where Eg is the band gap value determined through the UV absorption spectrum. The high frequency dielectric constant of the materials is a very important parameter for calculating the physical or electronic properties of materials. All the above parameters as estimated are shown in Table 1.

Table 1: Electronic parameters of the silver oxide nanoparticles

| Parameters | Value |
|---|---|
| Plasma energy ($h\omega_p$) | 17.512 eV |
| Penn gap ($E_p$) | 4.90 eV |
| Fermi Energy ($E_F$) | 13.393 eV |
| Electronic polarizability (using the Penn analysis) | 5.242 x $10^{-24}$ $cm^3$ |
| Electronic polarizability (using the Clausius-Mossotti relation) | 5.754 x $10^{-24}$ $cm^3$ |
| Electronic polarizability (using bandgap) | 5.989 x $10^{-24}$ $cm^3$ |

The silver oxide nanoparticles are placed in the heater and their response is taken at different temperatures. Temperature dependent dielectric constant and dielectric loss has been plotted in Figs. 8 and 9. It is also observed that as the temperature increases, the dielectric constant also increases to a considerable value as seen in Fig. 5. The same trend is observed in the case of dielectric loss versus temperature as well given in Fig. 6. The

behavior of dielectric properties with temperature is different over different temperature ranges i.e. at low and high temperature. It is evident from the Fig.8 and 9 that the dielectric constant and dielectric loss are low at a certain room temperature range and remain independent of temperature changes. In high temperature range the dielectric properties rise suddenly and reach a maximum value. The basic reason of the independency of dielectric constant in low temperature range is that impurities remain localized in this range and so conduction is not easy while at high temperature impurities are no more localized and hence conductivity of the material is increased. In case of ionic solids, electrons of the material also become free and contribute to conduction. This results in high polarization of the material; hence value of dielectric constant is increased with increase in temperature. At low and room temperature range, the effect of grain boundaries is dominant and that is why the dielectric properties have small magnitudes and are constant. As the temperature is increased, the role of grains becomes more and more effective and increases in the dielectric properties [20].

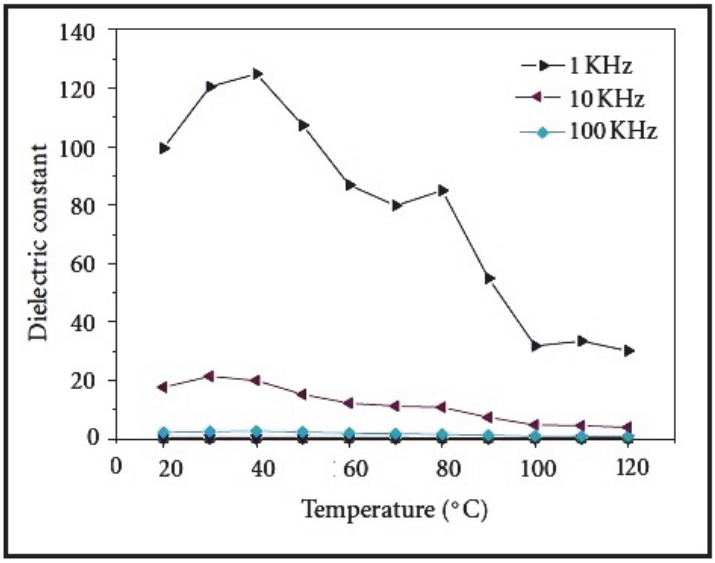


Fig. 8: Temperature dependent dielectric constant of silver oxide nanoparticles

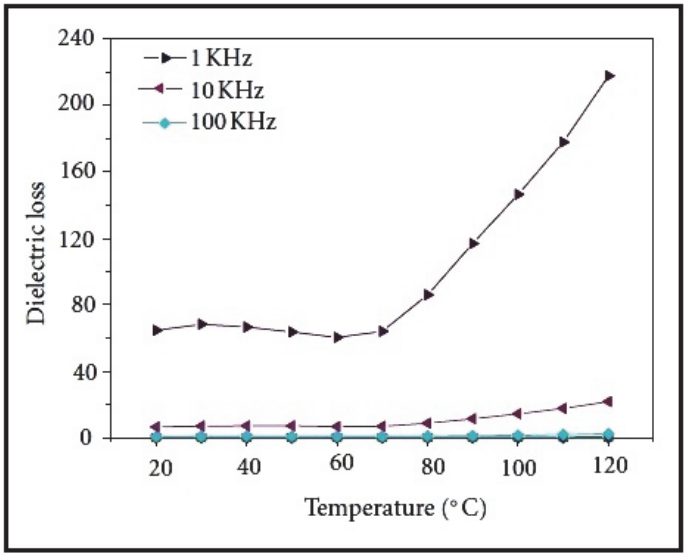


Fig. 9: Temperature dependent dielectric loss of silver oxide nanoparticles

The ac conductivity plot of the pelletized form of silver oxide nanoparticles is shown in Fig.10. It is observed from the results that the ac conductivity increases with the increase in temperature, which shows the semiconducting nature of the silver oxide nanoparticles. Due to the thermionic emission and tunnelling of charge carriers across the barrier, the conductivity increases with the temperature. Because of small size of the particles, the charge carriers reach the surface of the particles more and easily enabling the electron transfer by thermionic emission or tunneling to enhance the conductivity [21]. The a.c. conductivities strongly depend on the particle size, the concentration and heat treatment of the sample and the premelting of the electrolytes. Also, the frequency dependent data indicated that the enhancement was due to grains rather than grain boundary or surface conduction. The nature of frequency and temperature dependence of a.c. conductivity of the present samples, suggests an electronic hopping mechanism, exhibited by a large number of nanocrystalline materials. This hopping mechanism is compatible with the highly disordered or amorphous structure of the grain boundary layers of nanophase materials, having high densities of localized levels. This polarization, which is out of phase with the applied electric field, is measured as a.c. conductivity.

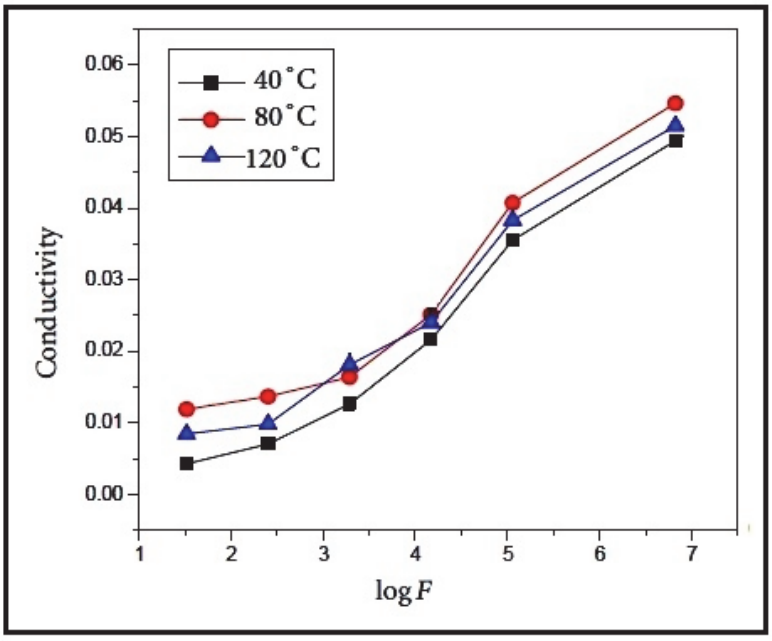


Fig.10: Variation of conductivity with log f

## 5. Conclusion

Silver oxide ($Ag_2O$) nanoparticles have been successfully synthesized using a wet chemical technique. X-ray diffraction analysis reveals that the crystallite size of the silver oxide particles was found to be 18.6 nm. Spherical shapes morphology of the prepared silver oxide nanoparticles was observed in the SEM studies. The transmission electron microscopic analysis confirms the prepared silver oxide nanoparticles with the particle size of around 19 nm. Absorption spectrum revealed that the extended absorption wavelength towards the visible-light region. The value of band gap energy obtained from UV absorption spectrum is 4.70 eV, which was also attributed to the formation of nanocrystalline silver oxide particles. The variation of dielectric constant, dielectric loss with frequency and temperature for silver oxide nanoparticles were analyzed. In addition, the plasma energy of

the valence electron, Penn gap or average energy gap, the Fermi energy and electronic polarizability of the silver oxide nanoparticles have been also determined. AC electrical conductivity was found to increase with an increase in the temperatures and frequency.

## References


[1] Y.L. Wu, A.I.K. Tok, F.Y.C. Boey, X.T. Zeng, X.H. Zhang, Appl.Surface Sci. **253** (2007) 5473.
[2] S.R. Lee, M.M. Rahman, M. Ishida and K. Sawada. Biosens. Bioelectron., **24** (2009) 1877-1882.
[3] A. Dıaz-Parralejo, R. Caruso, A.L. Ortiz and F. Guiberteau. Thin Sol. Film, **458** (2004) 92–97.
[4] S.R. Lee, M.M. Rahman, M. Ishida and K. Sawada. Trends in Anal. Chem., **28** (2009) 196-203.
[5] G.A.E. Mostafa and A. Al-Majed., J. Pharmaceut. Biomed. Anal., **48** (2008) 57–61.
[6] C. Feldmann, H.O. Jungk, Angew. Chem. Int. Ed. **40** (2001) 359.
[7] Y. Her, Y. Lan, W. Hsu and S. Y. Tsai, J. Appl. Phys, **96** (2004) 1283.
[8] J. Tominaga, J. Phys.: Condens. Matter, **15** (2003) R1101.
[9] B. E. Breyfogle, C. Hung, M. G. Shumsky and J. A. Switzer, J. Electrochem. Soc., **143** (1996) 2741.
[10] S.Suresh, International Journal of Physical Sciences, **9** (2014) 380-385
[11] Suresh Sagadevan, International Journal of Physical Sciences, **8** (2013) 1121-1127
[12] Suresh Sagadevan, American Journal of Nanoscience and Nanotechnology. **1** (2013) 27-30
[13] Suresh Sagadevan, Nanomaterials & Molecular Nanotechnology. **1** (2015) 1-4
[14] Sagadevan Suresh, International journal of Physical Sciences, **8** (21) (2013) 1121-1127
[15] N.M.Ravindra, R.P.Bharadwaj, K.Sunil Kumar, V.K.Srivastava, Infrared Phys. **21** (1981) 369–381
[16] V.Kumar, B.S.R Sastry, J. Phys. Chem. Solids, **66** (2005)99–102
[17] D.R.Penn, Phys. Rev. **128** (1962) 2093–2097
[18] N.M.Ravindra,V.K. Srivastava , Infrared Phys. **20** (1980) 399–418
[19] R.R.Reddy, Y.Nazeer Ahammed ,M. Ravi Kumar, J. Phys. Chem. Solids **56** (1995) 825–829
[20] S. Suresh, C. Arunseshan, Appl Nanosci. **4** (2014) 179–184
[21] Sagadevan Suresh, Appl Nanosci. **4** (2014) 325–329